Detection of Mechanical Prosthetic Valve Dysfunction

Manuela Muratori, MD[a,*], Laura Fusini, MD[a], Sarah Ghulam Ali, MD[a], Giovanni Teruzzi, MD[a], Nicoletta Corrieri, MD[a], Paola Gripari, PhD, MD[a], Massimo Mapelli, MD[a], Andrea Annoni, MD[a], Gloria Tamborini, MD[a], Mark G. Rabbat, MD[b,c], Gianluca Pontone, MD[a], Francesco Alamanni, MD[a,d], Piero Montorsi, MD[a,d], and Mauro Pepi, MD[a]

The long-term outcome of mechanical aortic and mitral prosthetic valve (A-PV, M-PV) dysfunction (PVD) remains a serious complication associated with high morbidity and mortality. We sought to evaluate the incremental diagnostic value of combined transthoracic echocardiography (TTE) and fluoroscopy (F) in patients with suspected PVD. A total of 354 patients (178 A-PV, 176 M-PV) were imaged by TTE and F within 5 days of hospital admission. PVD was confirmed by transesophageal echocardiography, computed tomography, effective thrombolysis, or surgical inspection. PVD was confirmed in 101 patients (57%) with M-PV and 99 (55%) with A-PV. Regardless of the mechanism of PVD, TTE shows good sensitivity and specificity, with accuracy of 80% for M-PV and 91% for A-PV. F shows high specificity, but low sensitivity with accuracy of 68% for M-PV and 78% for A-PV. The integration of TTE + F significantly improved accuracy both for M-PV (83%) and A-PV (96%). At ROC analysis, the combined model of TTE + F showed the highest area under the curve for the detection of PVD compared with TTE and F alone ($p < 0.001$). In conclusion, in patients with a clinical suspicion of PVD, the combined model of TTE + F offers incremental value over TTE or F alone. This multimodality imaging approach overcomes limitations of TTE or F alone and provides prompt identification of patients who may require further imaging assessment and/or closer follow up. **(Am J Cardiol 2021;00:1−9)**

The long-term outcome of mechanical aortic and mitral prosthetic valves (A-PV and M-PV) has greatly improved. Nevertheless, PV dysfunction (PVD) remains a very serious and challenging complication, associated with high mortality and morbidity.[1,2] Several studies have investigated the etiology of PVD, showing that the development of thrombosis, pannus or paraprosthetic regurgitation being closely related to PV failure,[3,4] The clinical presentation may vary from no symptoms to acute heart failure and sudden cardiac arrest, and the time between valve replacement and PVD may be very broad. Currently, transthoracic echocardiography (TTE) is the first-line imaging modality for the assessment of patients with PV. Transesophageal echocardiography (TEE) can better define the cause of PVD and help in guiding therapy, risk stratification and follow-up.[5,6] Computed tomography (CT) has recently emerged as a complementary approach offering excellent spatial resolution to identify a range of PV complications, including pannus formation.[7] Although TEE and CT are considered the gold-standard in the diagnosis of PVD,[8] an integrated multimodality imaging approach comprising several parameters by TTE and fluoroscopy (F) is essential to appropriately refer suspected PVD to TEE or CT and to devise the optimal therapeutic pathway. The aims of this study were: 1) to evaluate the incremental diagnostic value of combined TTE derived parameters and F over each imaging modality alone in symptomatic patients with high clinical suspicion of PVD, 2) to provide the basis for developing an algorithm allowing for rapid PVD diagnosis.

Methods

We retrospectively enrolled 354 patients with suspected PVD, admitted between 2000 and 2019 to Centro Cardiologico Monzino IRCCS (Milan, Italy). Symptoms of suspected PVD were dyspnea, cerebral and/or peripheral embolism, infective-like disease or hemolytic anemia. All patients underwent TTE, F and TEE within 5 days after hospital admission. Since 2010, 3D TEE was included in the standard diagnostic work-up and since 2013, patients with suspected PVD underwent also CT imaging. The gold standard for establishing PVD was the surgical inspection or effective thrombolysis and, when those were not available, the 2D/3D TEE imaging combined to CT data were used. The Ethical Committee of our institution approved the study (R1264/20-CCM 1328).

Normal PV function (N-PVF) was defined at TEE as the absence of obstructive or non-obstructive thrombus, vegetation or pannus ingrowth with normal leaflet(s) motion, and trivial PV regurgitation. Obstructive PVD (O-PVD) could be due to the presence of thrombus or pannus. Thrombus was defined by the evidence of irregular shaped mobile masses with low echogenicity at 2D/3D TEE and by low-

[a]Department of Cardiovascular Imaging, Centro Cardiologico Monzino IRCCS, Milan, Italy; [b]Division of Cardiology, Loyola University of Chicago, Chicago, IL; [c]Edward Hines Jr. VA Hospital, Hines, IL; and [d]Department of Clinical Sciences and Community Health, Cardiovascular Section, University of Milan, Milan, Italy. Manuscript received February 9, 2021; revised manuscript received and accepted March 30, 2021.

See page 8 for disclosure information.

*Corresponding author: Tel: 0039 0258002011, fax: 0039 0258002287.

E-mail address: manuela.muratori@centrocardiologicomonzino.it (M. Muratori).

0002-9149/
https://doi.org/10.1016/j.amjcard.2021.03.055

attenuation lesions ranging between 90 and 145 HU, starting in the valve ring area and then spreading to the leaflet(s) at CT. Pannus ingrowth was defined as a mass with lower area and lower density than thrombus at TEE, and as a low-attenuation lesion or a calcified lesion ≥145 HU, protruding into the valvular strut, beneath the PV at CT.[9-11] At surgical inspection thrombus was confirmed as a mobile mass more commonly located on the atrial side of M-PV and on the aortic root side of A-PV, and pannus was confirmed as a fibrotic ingrowth frequently seen on the ventricular side of M-PV and A-PV. In case of O-PVD, thrombolysis was carried out when thrombotic prosthetic mass size was <0.8 cm^2 at TEE. The results of the thrombolysis were defined as "full success" (leaflet motion normalization), "partial success" (improvement without normalization of leaflet motion), and "ineffective" (absence of improvement of the leaflet motion) using F.[4] Paraprosthetic valve dysfunction (P-PVD) was defined as paraprosthetic regurgitation with an echo-free space close to the sewing ring at TEE, leak by the contrast medium at CT or by surgical inspection.

Comprehensive TTE evaluation was performed using commercially available equipment (Sonos 7500, iE33 or EPIQ system, Philips Medical Systems, Andover, MA, USA; and Vivid 7 or E9, GE Healthcare, Horten, Norway). Multiple cross-sectional and off-axis views were performed to visualize the mobility of PV leaflet(s). Color Doppler was used for screening and evaluating the degree of intra and/or paraprosthetic regurgitation. Doppler-derived parameters in M-PV evaluation included: early peak mitral velocity (E wave), mean transprosthetic gradient (ΔP_{mean}), pressure half time, and Doppler velocity index (DVI).[8,12,13] Doppler-derived parameters in A-PV evaluation included: peak transprosthetic velocity (V_{max}), peak and mean transprosthetic gradients (ΔP_{max} and ΔP_{mean}), DVI, effective prosthetic orifice area, acceleration time (AT), ejection time (ET), and the ratio AT/ET.[8,14,15]

F was carried out with the patient in the supine position. Due to surgical PV orientation, multiple projections (0-90°) were performed, including cranial-caudal angulations. The examination was considered successful when the tilting disc projection (with the radiographic beam parallel to both the valve ring plane and the tilting axis of discs) was obtained and allowed calculation of opening and closing angles**.** Short F film (3−10 beats) at 50 frames/s was recorded. Frames of interest were selected to mesure disc(s) motion. For bileaflet prostheses, opening and closing angles were calculated as the distance between the 2 leaflets in the fully open and closed position. For the single disc prostheses, the opening angle was defined as the distance between the housing and the disc at its full open position.[2] Normal reference values for opening and closing angles were obtained from the manufacturer and used to evaluate leaflet motion, specifically for each prosthesis size and type.[16]

The TEE studies were performed using standard, commercially available systems (Sonos 7500, iE33, or EPIQ system, Philips Medical System, Andover, MA) with a 5 MHz multiplane probe or X7-2t probe. TEE examination included 2D and 3D conventional and off-axis views.

All CT examinations were performed using a 256-slice wide volume coverage scanner (Revolution CT, GE Healtcare, Milwaukee). CT scan was performed using an iterative reconstruction algorithm (ASIR-V; GE Healthcare) at 50% level, 100 kV tube voltage and a body-mass index adapted protocol for the tube current. A 16-cm scan volume including the whole cardiac volume during one single-heart beat was used with prospective ECG-gating. All patients received a 50mL bolus of contrast medium (Iomeprol, 400 mg/mL, Bracco, Milan, Italy) at an infusion rate of 5 mL/s followed by 50 mL of saline solution at 5 mL/s. CT dataset were post-processed on a dedicated workstation (Advantage Workstation Volume Share 4.6, GE Healthcare), with specific dedicated software enabling reconstruction of the aortic root in different orthogonal planes.

Based on the definition of PVD given for each imaging modality, the presence of PVD was retrospectively assessed by 2 cardiologists with more than 10 years of experience for analyzing the TTE and 2D/3D TEE data (M.M. and G. T.), by 2 interventional cardiologists for F data (G.T. and P. M.) and by 2 radiologists for CT data (A.A. and G.P.). The different experts were blinded to each other. Discrepancies between the 2 observers were resolved using joint reanalysis and discussion, and consensus values were used for statistics.

Continuous variables were presented as mean ± SD and categorical variables as absolute numbers and percentages. Analysis of variance for independent measurements were used to assess differences between the study subgroups. The association between categorical variables was examined using χ^2 test. A post hoc analysis for significant results were performed using the Bonferroni correction. Receiver operating characteristic curves (ROC) were computed to determine the optimal threshold for TTE, F and TTE + F to diagnose PVD using the Youden index and the area under the curves (AUC) were compared with the DeLong Method. All results were considered significant with P value <0.05. Statistical analysis was performed with SPSS, version 25 software (SPSS Inc, Chicago, IL) and R version 3.5.1.

Results

The study population comprised of 354 patients with suspected PVD (63±11years, 127 [36%] male; 178 A-PV and 176 M-PV) and were classified into 3 groups according to PV function (154 N-PVF, 131 O-PVD, and 69 P-PVD) as detected by the combined information from 2D TEE (n = 341), 3D TEE (n = 101), CT (n = 87), surgical inspection (n = 105), or thrombolysis response (n = 34). Main clinical characteristics of M-PV and A-PV are summarized in Table 1**.** Both in M-PV and A-PV, clinical parameters were similar between groups, except that NYHA III-IV was significantly more frequent in O-PVD and P-PVD and hemolytic anemia was significantly more frequent in P-PVD. INR was in range in all patients.

F was feasible in 95% of A-PV (93% of single disc PV, 95% of bileaflet PV) and in 89% of M-PV (83% of single disc PV, 91% of bileaflet PV). Opening and closing angles at F are reported in Table 2. In particular, F examination showed abnormal leaflet motion in 104 out of 131 patients with O-PVD (79%). opening and closing angles were not significantly different in P-PVD as compared to N-PVF.

Echocardiographic parameters are reported in Table 3 for M-PV and A-PV.

Table 1
Baseline clinical characteristics of the study population for prosthetic valves implanted in the mitral position and in the aortic position

	Mitral prosthetic valve(n = 176)				Aortic prosthetic valve(n = 178)			
Variable	N-PVF(n = 75)	O-PVD (n = 57)	P-PVD (n = 44)	p-value	N-PVF(n = 79)	O-PVD (n = 74)	P-PVD (n = 25)	p value
Age (year)	61 ± 11	65 ± 11	65 ± 9	0.030	66 ± 9	65 ± 12	62 ± 11	0.292
Male	15 (20%)	12 (21%)	18 (41%)*,†	0.026	42 (53%)	23 (31%)*	17 (68%)†	0.012
BSA (m2)	1.7 ± 0.18	1.73 ± 0.24	1.74 ± 0.19	0.427	1.79 ± 0.21	1.72 ± 0.18	1.84 ± 0.18†	0.009
NYHA functional class III-IV	9 (12%)	34 (60%)*	34 (77%)*	<0.001	6 (8%)	30 (41%)*	11 (44%)*	<0.001
Symptoms								
Dyspnea	67 (89%)	43 (75%)	34 (77%)	0.081	73 (92%)	69 (93%)	19 (76%)*,†	0.029
Embolic event	2 (3%)	5 (9%)	1 (2%)	0.175	0	2 (3%)	0	0.241
Infective-like disease	4 (5%)	8 (14%)	3 (7%)	0.186	5 (6%)	3 (4%)	5 (20%)*,†	0.027
Hemolytic anemia	2 (3%)	1 (2%)	6 (14%)*,†	0.012	1 (1%)	0	1 (4%)	0.257
INR	2.75 (2.19;3.35)	2.16 (1.92;3.40)	2.61 (2.10;3.33)	0.451	2.59 (2.12;3.16)	2.48 (2.07;3.03)	2.59 (2.03;3.28)	0.962
Rhythm				0.808				0.227
Sinus Rhythm	18 (24%)	11 (19%)	10 (23%)		47 (60%)	35 (49%)	15 (65%)	
Atrial Fibrillation	57 (76%)	46 (81%)	34 (77%)		31 (40%)	37 (51%)	8 (35%)	
A-PV plus M-PV	35 (47%)	18 (32%)	20 (45%)	0.181	33 (42%)	31 (42%)	6 (24%)	0.239
Coronary artery disease	1 (1%)	5 (9%)	3 (7%)	0.132	17 (22%)	10 (14%)	7 (28%)	0.215
Prosthetic type				0.363				0.873
Single disk	15 (20%)	9 (16%)	12 (27%)		13 (16%)	10 (13%)	4 (16%)	
Bileaflet	60 (80%)	48 (84%)	32 (73%)		66 (84%)	64 (87%)	21 (84%)	
Time from implantation (years)	14 (7;22)	15 (12;21)	21 (10;25)	0.513	13 (8;19)	12 (9;17)	8 (2;20) †	0.003

A-PV = Aortic Prosthetic Valve; M-PV = Mitral Prosthetic Valve; INR = international normalized ratio; NYHA = New York Heart Association; N-PVF = normal prosthetic valve function; O-PVD = obstructive prosthetic valve dysfunction; P-PVD = paraprosthetic valve dysfunction.

Post-hoc comparison (Bonferroni):

* $p < 0.05$ vs N-PVF;

† $p < 0.05$ vs O-PVF.

In M-PV, O-PVD and P-PVD showed higher ΔP_{mean}, DVI and E wave compared to N-PVF. Whereas, pressure half time was significantly higher only in O-PVD. In A-PV, O-PVD and P-PVD showed higher V_{max}, ΔP_{max} and ΔP_{mean} compared to N-PVF. DVI and effective prosthetic orifice area were lower and AT was higher in O-PVD compared to N-PVF and P-PVD. Both in M-PV and A-PV, left ventricular ejection fraction was similar among groups, but P-PVD had higher left ventricular and left atrial volumes. Moreover, O-PVD and P-PVD featured higher pulmonary artery systolic pressure compared with N-PVF.

Regardless of PVD, TTE shows good sensitivity and specificity, with diagnostic accuracy of 91% for A-PV and 80% for M-PV (Table 4). F shows a very high specificity (100% for M-PV and 99% A-PV), but a low sensitivity (46% for M-PV and 62% A-PV) and a diagnostic accuracy

Table 2
Fluoroscopic opening and closing angles for single disk and bileaflet aortic and mitral prosthetic valves according to the groups of prosthetic valve function

		N-PVF	O-PVD	P-PVD	p value
Mitral Prosthetic Valve	Single disk (n = 36)	(n = 9/15)	(n = 9/9)	(n = 12/12)	
	Opening Angle (°)	64 ± 6	42 ± 13*	65 ± 10†	<0.001
	Closing Angle (°)	0 ± 0	5 ± 6	3 ± 5	0.170
	Bileaflet (n = 140)	(n = 56/60)	(n = 42/48)	(n = 29/32)	
	Opening Angle (°)	18 ± 5	56 ± 30*	19 ± 8†	<0.001
	Closing Angle (°)	127 ± 9	132 ± 6*	126 ± 10†	0.031
Aortic Prosthetic Valve	Single disk (n = 27)	(n = 11/13)	(n = 10/10)	(n = 4/4)	
	Opening Angle (°)	57 ± 7	47 ± 3*	59 ± 2†	<0.001
	Closing Angle (°)	0 ± 0	2 ± 5	3 ± 6	0.247
	Bileaflet (n = 151)	(n = 62/66)	(n = 61/64)	(n = 21/21)	
	Opening Angle (°)	18 ± 5	41 ± 21*	18 ± 7†	<0.001
	Closing Angle (°)	129 ± 9	126 ± 10	130 ± 7	0.163

N-PVF = normal mitral prosthetic valve function; O-PVD = obstructive prosthetic valve dysfunction; P-PVD: paraprosthetic valve dysfunction.

Post-hoc comparison (Bonferroni):

* $p < 0.05$ vs N-PVF;

† $p < 0.05$ vs O-PVF.

Table 3
Echocardiographic characteristics of patients with mitral and aortic prosthetic valves

Mitral Prosthetic Valve	N-PVF(n = 75)	O-PVD (n = 57)	P-PVD (n = 44)	p Value
ΔPmean (mm Hg)	5 ± 2	10 ± 6*	7 ± 2	<0.001
DVI (VTIM-PV/VTILVOT)	1.8 ± 0.4	3.2 ± 1.6*	2.6 ± 0.5*,†	<0.001
E wave (m/s)	189 ± 31	227 ± 46*	231 ± 35*	<0.001
PHT (ms)	90 ± 29	175 ± 81*	101 ± 34†	<0.001
LVEF (%)	57±12	55±13	55±9	0.602
LVEDV (mL)	105 ± 49	99 ± 56	133 ± 49*,†	0.003
LVESV (mL)	49 ± 41	49 ± 48	62 ± 32*,†	0.002
LA volume index (mL/m2)	81 ± 47	87 ± 54	99 ± 40	0.317
PAPS (mm Hg)	38 ± 11	49 ± 15*	55 ± 16*	<0.001
Aortic Prosthetic Valve	**N-PVF(n = 79)**	**O-PVD (n = 74)**	**P-PVD (n = 25)**	**p value**
Vmax (m/s)	2.6 ± 0.6	3.9 ± 0.8*	3.3 ± 0.6*,†	<0.001
ΔPmax (mm Hg)	28 ± 13	64 ± 26*	43 ± 15*,†	<0.001
ΔPmean (mm Hg)	16 ± 7	37 ± 16*	24 ± 10*,†	<0.001
DVI (VTILVOT/VTIA-PV)	0.4 ± 0.1	0.3 ± 0.1*	0.4 ± 0.1†	<0.001
AT (ms)	76 ± 16	101 ± 17*	83 ± 12†	<0.001
AT/ET (ms)	0.26 ± 0.05	0.33 ± 0.05*	0.27 ± 0.04†	<0.001
EOA (cm2)	1.57 ± 0.53	0.93 ± 0.26*	1.46 ± 0.44†	<0.001
EF (%)	57 ± 10	60 ± 11	53 ± 8†	0.005
LVEDV (mL)	111 ± 40	105 ± 39	165 ± 49*,†	<0.001
LVESV (mL)	51 ± 32	45 ± 32	78 ± 29*,†	<0.001
LA volume index (mL/m^2)	71 ± 37	71 ± 32	62 ± 21	0.872
PAPS (mm Hg)	36 ± 10	41 ± 11*	40 ± 11*	0.012

AT = acceleration time; ΔPmax = peak transprosthetic pressure gradient; ΔPmean = mean transprosthetic pressure gradient; DVI = Doppler velocity index; E wave = early peak mitral velocity; EDV = end diastolic volume; EF = ejection fraction; EOA = effective orifice area; ESV = left ventricular end systolic volume; ET = ejection time; LA = left atrial; LV = left ventricular; PAPS = pulmonary artery systolic pressure; PHT = pressure half time; Vmax = peak transprosthetic velocity; VTIA-PV = time velocity index of prosthetic aortic valve; VTILVOT = time velocity index of left ventricular outflow; VTIM-PV = time velocity index of prosthetic mitral valve.

Post-hoc comparison (Bonferroni):
* $p < 0.05$ vs N-PVF;
† $p < 0.05$ vs O-PVF.

of 68% for M-PV and 78% for A-PV. Figure 1 illustrates the combined model of TTE plus F defines the highest AUC for the detection of M-PVD and A-PVD compared with TTE and F alone.

Figure 2 summarizes PVD treatment according to different PVD diagnosis and clinical presentations. PVD was confirmed in 200 patients (56%), of which 101 M-PVD and 99 A-PVD. P-PVD was found in 69 patients, of which 45 cases (65%) were referred to surgery, with a mortality of 21% for the M-PV and of 7% for A-PV. Effective transcatheter closure of the paravalvular leak was performed in 4 patients with M-PV (6%). In the remaining 20 patients (29%) of the P-PVD group, a wait-and see approach was adopted. O-PVD was found in 131 patients, of which 34 cases (26%) underwent thrombolysis with full success in 12 M-PV (62%) and only in 1 A-PV (8%). Thrombolysis was partially effective in 15 cases (44%), ineffective in 6 patients (18%, 4 M-PV and 2 A-PV) with a mortality rate

Table 4
Diagnostic performance of TTE, F and TTE + F in detecting prosthetic valve dysfunction

	Mitral prosthetic valve			Aortic prosthetic valve		
Variable	TTE(n = 176)	F(n = 160)	TTE + F(n = 160)	TTE(n = 178)	F(n = 171)	TTE + F(n = 171)
True positive	82	45	85	89	59	95
True negative	58	63	48	73	74	69
False positive	17	0	15	6	1	6
False negative	19	52	12	10	37	1
Sensitivity, % (CI 95%)	81(73−89)	46(36−56)	88(81−94)	90(84−96)	61(52−71)	99(97−100)
Specificity, % (CI 95%)	77(68−87)	100(100−100)	76(66−87)	92(87−98)	99(96−100)	92(86−98)
Negative predictive value, %, (CI 95%)	75(66−85)	55(46−64)	80(70−90)	88(81−95)	67(58−75)	99(96−101)
Positive predictive value, % (CI 95%)	83(75−90)	100(100−100)	85(78−92)	94(89−99)	98(95−100)	94(89−99)
Accuracy, % (CI 95%)	80(74−86)	68(60−75)	83(77−89)	91(87−95)	78(72−84)	96(93−99)

CI = confidence interval; F = fluoroscopy; TTE = transthoracic echocardiography.

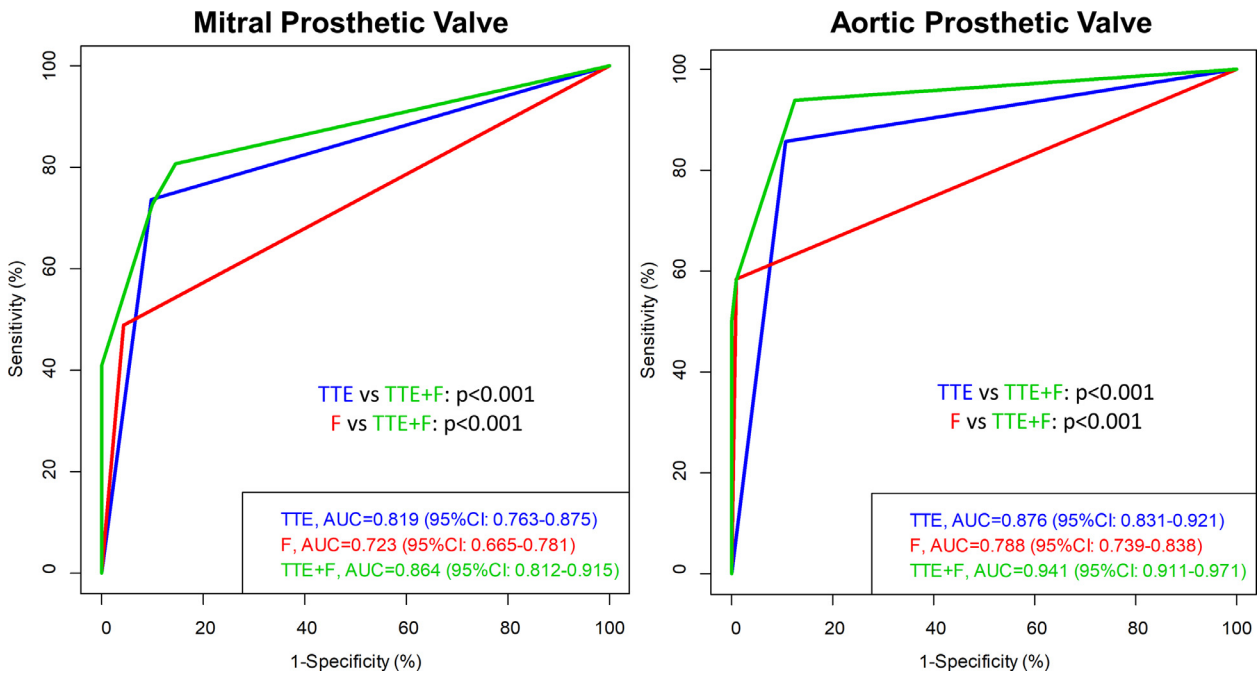

Figure 1. ROC analysis. Area under the curve (AUC) comparisons of the diagnostic performance to detect prosthetic valve dysfunction of transthoracic echocardiography (TTE), fluoroscopy (F) or combination of TTE + F for mitral prosthetic valve (left) and aortic prosthetic valve (right).

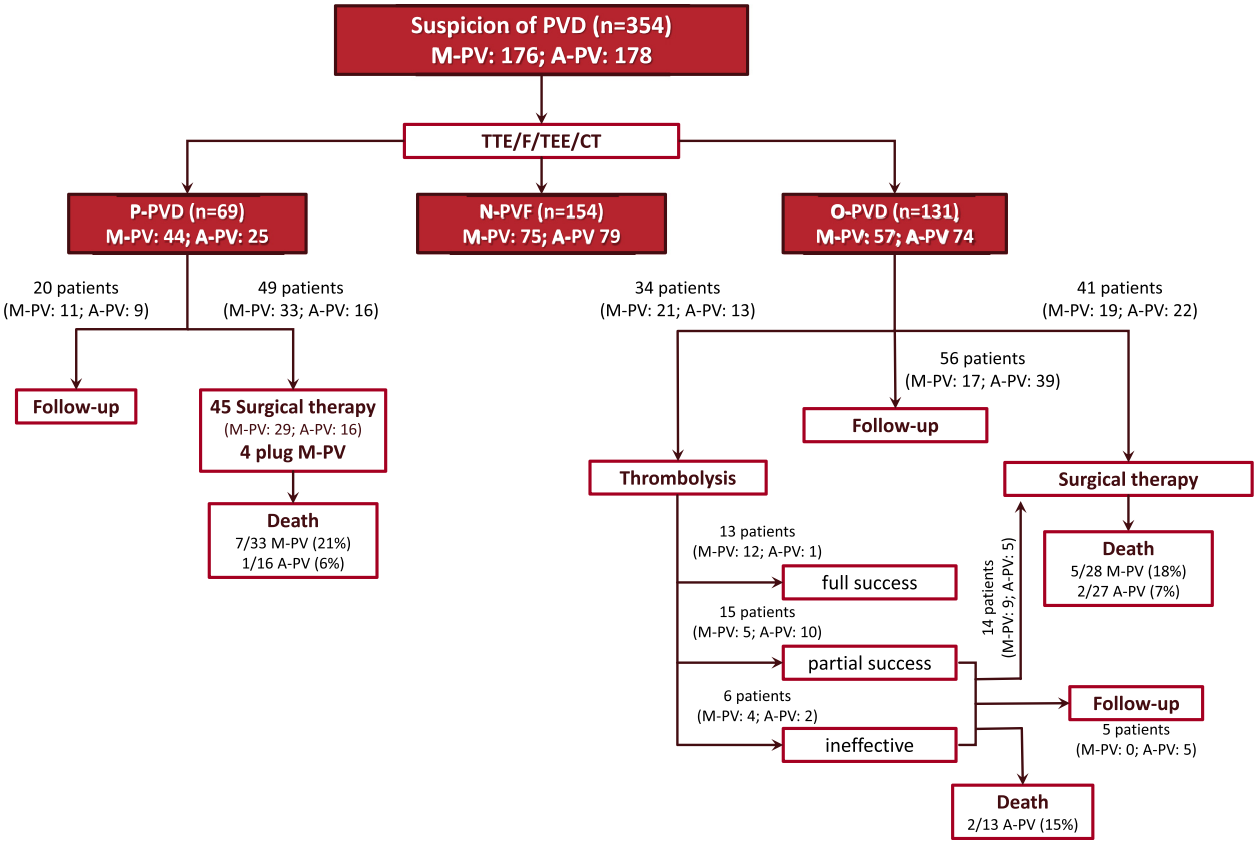

Figure 2. Treatment algorithm for patients with suspicion of prosthetic valve dysfunction. PVD, prosthetic valve dysfunction; M-PV, mitral prosthetic valve; A-PV, aortic prosthetic valve; TTE, transthoracic echocardiography; F, fluoroscopy; CT, computed tomography; P-PVD, paraprosthetic PVD; N-PVF, normal prosthetic valve function; O-PVD, obstructive PVD.

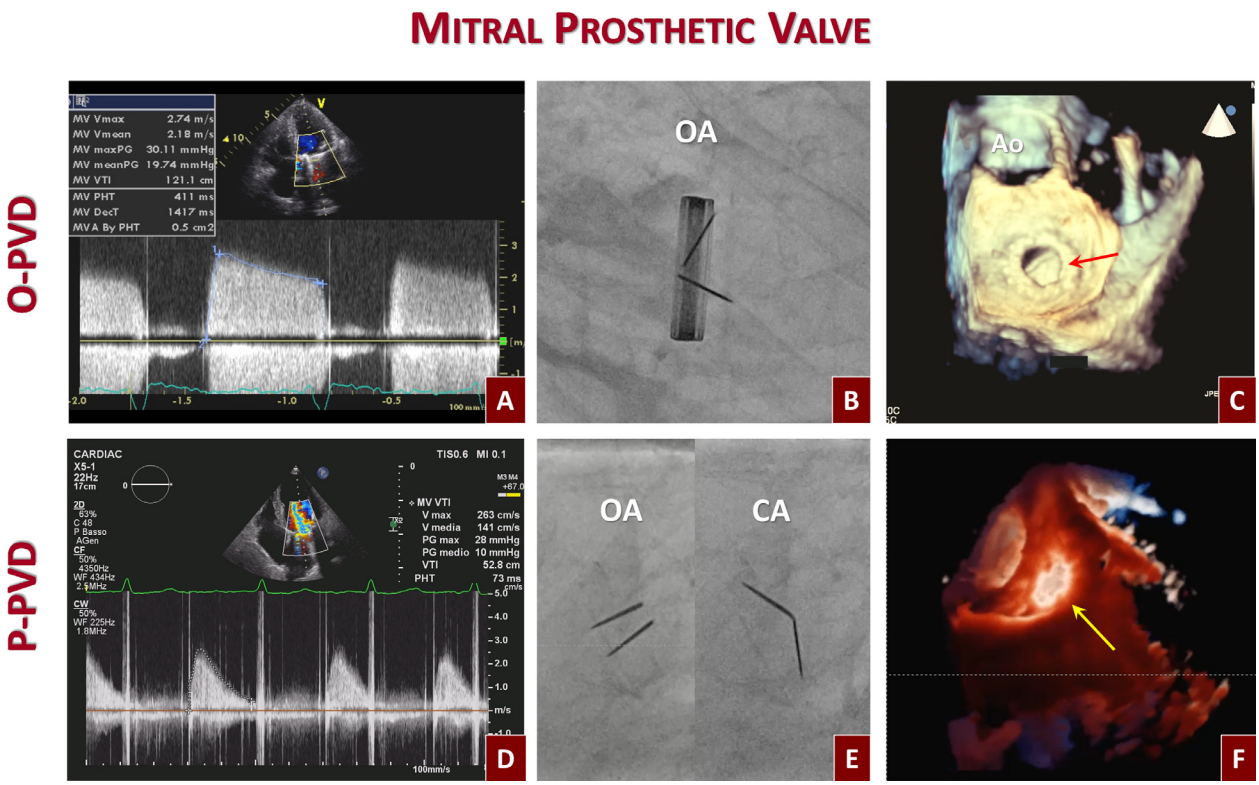

Figure 3. Examples of obstructive and paraprosthetic mitral valve dysfunction. Top. O-PVD: (A) high transprosthetic gradients and prolonged pressure half time detected by continuous Doppler TTE, (B) leaflet restriction at fluoroscopy and (C) at 3D TEE (red arrow). Bottom. P-PVD: (D) increased mitral peak E velocity and high mean transprosthetic gradient with normal pressure half time detected by Doppler TTE, (E) normal leaflet motion at fluoroscopy, and (F) paraprosthetic defect (yellow arrow) at 3D TEE (color version of figure is available online.).

of 0% for M-PV and 15% for A-PV. A total of 55 patients (42%) were referred to surgery with a mortality rate of 18% for M-PV and 7% for A-PV. In the remaining 56 pts (43%), a wait-and see approach was adopted. Figures 3 and 4 show examples of M-PVD and A-PVD, respectively.

Discussion

The main findings of this study are: 1) PVD is a serious complication of mechanical PV with a time of onset of about 10 years; 2) the integration of several TTE-Doppler parameters is essential for the detection of PVD; 3) the combined model of TTE + F provides the highest accuracy for the diagnosis of PVD compared to TTE and F alone.

Surgical valve replacement is currently the standard of care for treatment of valvular heart disease in patients at low and intermediate risk for surgery.[17,18] Mechanical PV are more durable compared to biological PV, but they are more thrombogenic. This implies the need for long-term anticoagulation therapy to prevent thrombosis, which can lead to disabling or fatal stroke.[10] In addition to thrombosis, pannus ingrowth and paravalvular leaks are serious complications in mechanical PV.

In our study, the time between valve replacement and the occurrence of PVD was about 10 years, except for aortic paravalvular leaks, which were observed significantly earlier (8 years). This is in accordance with the literature and the fact that TTE better identifies paravalvular leaks in A-PV, especially if in the anterior site. In M-PV, artifacts and acoustic shadowing may prevent TTE assessment of prosthetic leaks.[12] Moreover, O-PVD and P-PVD are equally represented in M-PVD; O-PVD is more frequent in A-PVD. Indeed, A-PV are more exposed to pannus ingrowth than M-PV (70% vs 21%).[19-22]

Current guidelines have highlighted the value of TTE Doppler parameters for PVD detection.[8,12] In M-PVD, DVI is one of the most useful parameters, providing a measure of PV function independent of cardiac output variation. Indeed, in the absence of aortic regurgitation and paying attention to matching cardiac cycles in atrial fibrillation, there is an expected proportional change in both VTI of M-PV and VTI of LVOT.[8,12,13] In O-PVD a high DVI reflects a significant increase in Doppler flow velocities proportional to a reduced effective prosthetic orifice area. In the presence of P-PVD, a high DVI reflects the disproportionate increase in flow across the PV, due to the regurgitant volume compared with left ventricular stroke volume.[13] In our study, combining DVI to the other TTE flow-dependent parameters, such as ΔP_{mean} and E wave, it was possible to identify M-PVD with an accuracy of 80%. Similarly, in A-PVD, combining traditional TTE−Doppler parameters (V_{max}, ΔP_{max} and ΔP_{mean}) with the ejection time parameters

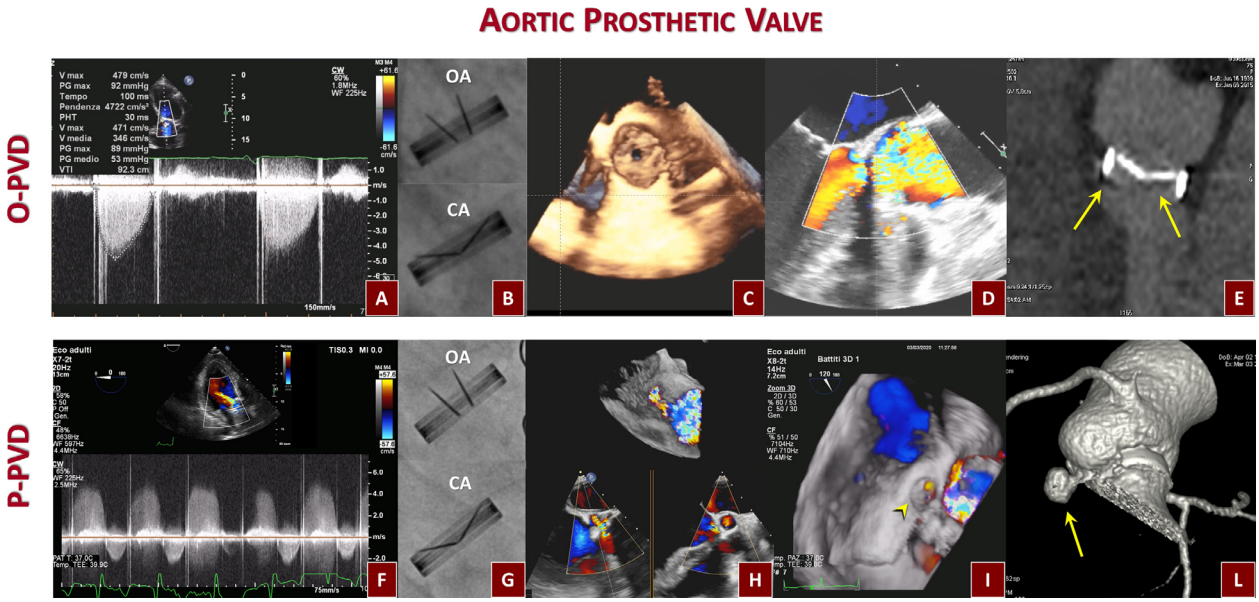

Figure 4. Examples of obstructive and paraprosthetic aortic valve dysfunction. Top. O-PVD: (A) high transprosthetic gradient documented with continuous wave Doppler by TTE, (B) abnormal opening and closing angle at fluoroscopy, (C) subaortic pannus at 3D TEE, (D) flow acceleration due to the subvalvular tissue at the level of the ring seen by color TEE, (E) pannus ingrowth (yellow arrows) as hypodense subprosthetic tissue on the ventricular side of the prosthesis detected by CT. Bottom. P-PVD: (F) holodiastolic regurgitation at continuous wave Doppler TTE, (G) normal leaflet motion at fluoroscopy, (H-I) pseudoaneurysm with paraprosthetic regurgitation assessed by 2D and 3D color TEE (yellow arrowhead), (L) pseudoaneurysm reconstructed by CT (color version of figure is available online.).

(AT and AT/ET) it was possible to identify A-PVD with an accuracy of 91%. Our data confirm previous studies reporting an accuracy of 94% of AT in the identification of O-PVD.[14,15] Moreover, high trans prosthetic gradients combined with normal ejection time parameters and normal DVI identified aortic P-PVD as confirmed by TEE.

Even though F does not allow hemodynamic assessment or provide clues about the etiology of reduced disc mobility,[8] it is a reliable, easy, and readily available technique to follow-up mechanical PV.[2,4,16] However, the different orientation given to the PV may represent a limitation of the technique accounting for unsatisfactory results when only "en face" visualization is feasible.[16] In our series, opening and closing angles were obtained in 89% of M-PV and in 95% of A-PV. In fact, A-PV are more frequently implanted in the antianatomic position allowing correct opening and closing angles measurements. In our study, F confirms a very high specificity in the identification of leaflet restriction, but a low sensitivity, with an overall accuracy of 68% in M-PV and 78% in A-PV. F was inaccurate in cases of non-obstructive thrombosis of M-PV (33% of false negative), as described also by Gueret et al[23] In A-PVD, F showed a low accuracy because subprosthetic pannus altered disc motion only when the circumferential involvement of the structure came close to 360˚ as demonstrated in our cases by CT or surgical inspection. This phenomenon has also been described in a recent biomedical engineering in vitro study,[22] that showed eccentric pannus with an involvement angle of 180˚ did not induce leaflet restriction while circumferential pannus decreased the opening angle from approximately 82˚ to 58˚. Moreover, F is not able to identify P-PVD both in M-PV and A-PV.

Despite the fact that TTE and F share good overall diagnostic performance, both have strengths and weaknesses that could be partially overcome by the integration of TTE + F. In fact, TTE + F have significantly higher AUC compared to each imaging modality alone. This allows for an early identification of PVD, thus giving the possibility to further assess patients with TEE or CT to devise the optimal treatment strategy.

Optimal management of PVD remains controversial and depends on an early identification of the patients needing further assessment. We demonstrated that in a large population of suspected PVD, the combined model of TTE + F not only provides prompt recognition of PVD, but also facilitates the identification of O-PVD vs P-PVD. In fact, the coexistence of altered Doppler parameters and normal leaflets dynamics will steer towards P-PVD. Conversely, the coexistence of altered Doppler parameters and altered leaflets dynamics will steer towards the O-PVD. Although these signals have to be confirmed by a second level imaging technique such as TEE and CT, TTE + F may facilitate the correct indication for TEE (suspicion of P-PVD) or CT (suspicion of O-PVD).

Lastly, even if therapeutic options in PVD are beyond the scope of our study, we confirmed that surgical management of PVD, despite the improvement in survival within the past decade, is associated with a significant death risk up to 20% in M-PVD and 7% in A-PVD, as similarly reported in recent studies.[24-26] However, thrombolysis has been confirmed to be a valid approach with lower mortality and complications than the surgical approach, if reserved to selected cases of mitral O-PVD, while it showed low efficacy and high mortality (15%) in aortic O-PVD. This

observation reinforced the importance of a detailed diagnostic work-up.

Our study has limitations. First, this is a retrospective study based on a cohort from a single tertiary center. Second, there was no independent echocardiography core lab. Finally, we did not routinely perform cardiac CT and 3D TEE that might have potentially supplied additional information in pannus/thrombus diagnosis and therefore we could not perform a head-to-head comparison with TTE and F in all cases.

In conclusion, mechanical PVD remains a challenging problem, with a high mortality regardless of treatment. In patients with symptoms of suspected PVD, the integration of TTE and F is a feasible and valuable strategy to assess PV function. This approach plays a pivotal role in diagnosis of relevant PVD and in the identification of patients who require further assessment with TEE or CT.

Author Contributions

Manuela Muratori: Conceptualization, Methodology, Data Curation, Writing - Original Draft, Project administration. Laura Fusini: Conceptualization, Methodology, Formal analysis, Writing - Original Draft, Visualization. Sarah Ghulam Ali: Data Curation, Investigation. Giovanni Teruzzi: Data Curation. Nicoletta Corrieri: Data Curation. Paola Gripari: Data Curation. Massimo Mapelli: Data Curation, Investigation. Andrea Annoni: Data Curation, Investigation. Gloria Tamborini: Data Curation, Writing - Review & Editing. Mark G. Rabbat: Writing - Review & Editing. Gianluca Pontone: Writing - Review & Editing. Francesco Alamanni: Data Curation, Writing - Review & Editing. Piero Montorsi: Conceptualization, Data Curation, Writing - Original Draft, Supervision. Mauro Pepi: Conceptualization, Methodology, Writing - Original Draft, Supervision, Visualization.

Disclosures

The authors declare that they have no known competing financial interests or personal relationships that could have appeared to influence the work reported in this paper.

1. Deviri E, Sareli P, Widenbaugh T, Cronje SL. Obstruction of mechanical heart valve prostheses: clinical aspects and surgical management. *J Am Coll Cardiol* 1991;17:646–650.
2. Montorsi P, De Bernardi F, Muratori M, Cavoretto D, Pepi M. Role of cine-fluoroscopy, transthoracic, and transesophageal echocardiography in patients with suspected prosthetic heart valve thrombosis. *Am J Cardiol* 2000;85:58–64.
3. Ionescu A, Fraser AG, Butchart EG. Prevalence and clinical significance of incidental paraprosthetic valvar regurgitation: a prospective study using transoesophageal echocardiography. *Heart* 2003;89:1316–1321.
4. Montorsi P, Cavoretto D, Alimento M, Muratori M, Pepi M. Prosthetic mitral valve thrombosis: can fluoroscopy predict the efficacy of thrombolytic treatment? *Circulation* 2003;108(Suppl 1):II79–II84.
5. Tong AT, Roudaut R, Ozkan M, Sagie A, Shahid MS, Pontes Júnior SC, Carreras F, Girard SE, Arnaout S, Stainback RF, Thadhani R, Zoghbi WA, Prosthetic Valve Thrombolysis-Role of Transesophageal Echocardiography (PRO-TEE) Registry Investigators. Transesophageal echocardiography improves risk thrombolysis of prosthetic valve thrombosis: results of the international PRO-TEE registry. *Am Coll Cardiol* 2004;43:77–84.
6. Pattabiraman V, Nanda NC, Iqbal F, Singh P, Koneru J, Akins C. Incremental value of three-dimensional over two-dimensionial transesophageal echocardiography in the assessment of acute dysfunction of mechanical mitral valve prosthresis. *Echocardiography* 2010;27:885–887.
7. Moss AJ, Dweck MR, Dreisbach JG, Williams M, Mak SM, Cartlidge T, Nicol ED, Morgan-Hughes GJ. Complementary role of cardiac CT in the assessment of aortic valve replacement dysfunction. *Open Heart* 2016;3:e000494.
8. Lancellotti P, Pibarot P, Chambers J, Edvardsen T, Delgado V, Dulgheru R, Pepi M, Cosyns B, Dweck MR, Garbi M, Magne J, Nieman K, Rosenhek R, Bernard A, Lowenstein J, Vieira ML, Rabischoffsky A, Vyhmeister RH, Zhou X, Zhang Y, Zamorano JL, Habib G. Recommendations for the imaging assessment of prosthetic heart valves: a report from the european association of cardiovascular imaging endorsed by the chinese society of echocardiography, the inter-american society of echocardiography, and the brazilian department of cardiovascular imaging. *Eur Heart J Cardiovasc Imaging* 2016;17:589–590.
9. Tanis W, Habets J, van der Brink RB, Symersky P, Budde RP, Chamuleau SA. Differentiation of thrombus from pannus as the cause of acquired mechanical prosthetic heart valve obstruction by non-invasive imaging: a review of the literature. *Eur Heart J Cardiovasc Imaging* 2014;15:119–129.
10. Dangas GD, Weitz JI, Giustino G, Makkar R, Mehran R. prosthetic heart valve thrombosis. *J Am Coll Cardiol* 2016;68:2670–2689.
11. Aladmawi MA, Pragliola C, Vriz O, Galzerano D. Use of multidetector-row computed tomography scan to detect pannus formation in prosthetic mechanical aortic valves. *J Thorac Dis* 2017;9:S343–S348.
12. Zoghbi WA, Chambers JB, Dumesnil JG, Foster E, Gottdiener JS, Grayburn PA, Khandheria BK, Levine RA, Marx GR, Miller FA Jr, Nakatani S, Quiñones MA, Rakowski H, Rodriguez LL, Swaminathan M, Waggoner AD, Weissman NJ, Zabalgoitia M. Recommendations for evaluation of prosthetic valves with echocardiography and doppler ultrasound: a report from the american society of echocardiography's guidelines and standards committee and the task force on prosthetic valves, developed in conjunction with the american college of cardiology cardiovascular imaging committee, cardiac imaging committee of the american heart association, the european association of echocardiography, a registered branch of the european society of cardiology, the japanese society of echocardiography and the canadian society of echocardiography, endorsed by the american college of cardiology foundation, american heart association, european association of echocardiography, a registered branch of the european society of cardiology, the japanese society of echocardiography, and canadian society of echocardiography. *J Am Soc Echocardiogr* 2009;22:975–1014.
13. Luis SA, Blauwet LA, Samardhi H, West C, Mehta RA, Luis CR, Scalia GM, Miller FA Jr, Burstow DJ. Usefulness of mitral valve prosthetic or bioprosthetic time velocity index ratio to detect prosthetic or bioprosthetic mitral valve dysfunction. *Am J Cardiol* 2017;120:1373–1380.
14. Ben Zekry S, Saad RM, Özkan M, Al Shahid MS, Pepi M, Muratori M, Xu J, Little SH, Zoghbi WA. Flow acceleration time and ratio of acceleration time to ejection time: novel diagnostic parameters for prosthetic aortic valve function. *J Am Coll Cardiol Imaging* 2011;4:1161–1170.
15. Muratori M, Montorsi P, Maffessanti F, Teruzzi G, Zoghbi WA, Gripari P, Tamborini G, Ghulam Ali S, Fusini L, Fiorentini C, Pepi M. Dysfunction of bileaflet aortic prosthesis: accuracy of echocardiography versus fluoroscopy. *JACC Cardiovasc Imaging* 2013;6:196–205.
16. Montorsi P, Cavoretto D, Repossini A, Bartorelli AL, Guazzi MD. Valve design characteristics and cine-fluoroscopic appearance of five currently available bileaflet prosthetic heart valves. *Am J Card Imaging* 1996;10:29–41.
17. Nishimura RA, Otto CM, Bonow RO, Carabello BA, Erwin JP 3rd, Guyton RA, O'Gara PT, Ruiz CE, Skubas NJ, Sorajja P, Sundt TM 3rd, Thomas JD, ACC/AHA Task Force Members. 2014 AHA/ACC guideline for the management of patients with valvular heart disease: executive summary: a report of the American College of Cardiology/American Heart Association Task Force on Practice Guidelines. *Circulation* 2014;129:2440–2492.
18. Nishimura RA, Otto C, Bonow RO, Carabello BA, Erwin JP 3rd, Fleisher LA, Jneid H, Mack MJ, McLeod CJ, O'Gara PT, Rigolin VH, Sundt TM 3rd, Thompson A. 2017 AHA/ACC focused update of the 2014 AHA/ACC guideline for the management of patients with valvular heart disease: a report of the American College of Cardiology/

American Heart Association Task Force on Clinical Practice Guidelines. *J Am Coll Cardiol* 2017;70:252–289.

19. Barbetseas J, Nagueh SF, Pitsavos C, Toutouzas PK, Quinones MA, Zoghbi WA. Differentiating thrombus from pannus formation in obstructed mechanical prosthetic valves: an evaluation of clinical, transthoracic and transesophageal echocardiographic parameters. *J Am Coll Cardiol* 1998;32:1410–1417.
20. Rizzoli G, Guglielmi C, Toscano G, Pistorio V, Vendramin I, Bottio T, Thiene G, Casarotto D. Reoperations for acute prosthetic thrombosis and pannus: an assessment of rates, relationship and risk. *Eur J Cardiothorac Surg* 1999;16:74–80.
21. Oh SJ, Park S, Kim JS, Kim KH, Kim KB, Ahn H. Reoperation for non-structural valvular dysfunction caused by pannus ingrowth in aortic valve prosthesis. *J Heart Valve Dis* 2013;22:591–598.
22. Ha H, Koo HJ, Hu HK, Kim GB, Kweon J, Kim N, Kim YH, Kang JW, Lim TH, Song JK, Lee SJ, Yang DH. Effect of pannus formation on the prosthetic heart valve: In vitro demonstration using particle image velocimetry. *PLoS One* 2018;13:e0199792.
23. Gueret P, Vignon P, Fournier P, Chabernaud JM, Gomez M, LaCroix P, Bensaid J. Transesophageal echocardiography for the diagnosis and management of nonobstructive thrombosis of mechanical mitral valve prosthesis. *Circulation* 1995;91:103–110.
24. Huang G, Schaff HV, Sundt TM, Rahimtoola SH. Treatment of obstructive thrombosed prosthetic heart valve. *J Am Coll Cardiol* 2013;62:1731–1736.
25. Sorajja P, Cabalka AK, Hagler DJ, Rihal CS. Long-term follow-up of percutaneous repair of paravalvular prosthetic regurgitation. *J Am Coll Cardiol* 2011;58:2218–2224.
26. Castilho FM, De Sousa MR, Mendonça AL, Ribeiro AL, Cáceres-Lóriga FM. Thrombolytic therapy or surgery for valve prosthesis thrombosis: systematic review and meta-analysis. *J Thromb Haemost* 2014;12:1218–1228.